The calcium isotopic composition of carbonate hardground cements: A new record of changes in ocean chemistry?

Andrea M. Erhardt, Alexandra V. Turchyn, Harold J. Bradbury, J.A.D. Dickson

Abstract

Reconstructing changes in the calcium isotopic composition ($\delta^{44}Ca$) of the ocean over Earth history has been challenging. This difficulty is due to the large range of calcium isotope fractionation factors during mineral precipitation and the potential for overwriting the initial $\delta^{44}Ca$ of minerals during shallow marine diagenesis. We present a new $\delta^{44}Ca$ record measured in carbonate hardground cements, an inorganic carbonate-mineral precipitate that rapidly forms at or near the sediment-water interface. The range in the $\delta^{44}Ca$ for any particular carbonate hardground cements is between 0.05 and 0.56‰. In some cases, the progressive increase in the $\delta^{44}Ca$ during precipitation can be observed, consistent with precipitation in a 'closed-system'. Our data show an average calcium isotope fractionation during carbonate hardground cement precipitation that is -0.57±0.27‰, similar to the calcium isotope fractionation factor for inorganic calcite precipitates in previous laboratory and modelling studies, and closer to what is considered a kinetic end member calcium isotope fractionation than growth at equilibrium. This is consistent with the rapid carbonate mineral precipitation expected for carbonate hardground cements. Our $\delta^{44}Ca$ record over the Phanerozoic is similar to other calcium-bearing mineral records over the same time interval, with average $\delta^{44}Ca$ becoming lower going back in time by about 0.5 to 0.7‰. Our results add further support for the evolution of seawater $\delta^{44}Ca$ over time, and we discuss the possible causes of these changes with suggestions for future studies.

Introduction

The growing interest in understanding the biogeochemical calcium cycle over geological time stems from the hope that, by reconstructing the calcium cycle, we will gain insight into the global carbon cycle (De La Rocha and DePaolo, 2000; Farkaš et al., 2007a; Blättler and Higgins, 2017). In principle, the dominant source of calcium to the global ocean, rivers through carbonate and silicate weathering, and the dominant sink for calcium from the global ocean, the deposition and lithification of carbonate-bearing sediments, are the same processes moving carbon through, to, and from Earth's surface environment (Fantle, 2010; Fantle and Tipper, 2014; Blättler and Higgins, 2017). If we could accurately reconstruct changes in these fluxes across Earth's surface environment over time, would we gain insight into the evolution of the carbon cycle that has, so far, eluded us?

The tool that has been most used to reconstruct the calcium cycle over time is the measurement of the calcium isotopic composition of calcium bearing minerals; particularly carbonate minerals (Farkaš et al., 2007a; Blättler et al., 2012). The calcium isotopic composition is reported as the ratio of the heavy ^{44}Ca isotope to the lighter ^{40}Ca isotope versus a standard in 'delta' notation, with units of parts per thousand, or permil.

$$\delta^{44}Ca = \left(\frac{{}^{44}Ca/{}_{^{40}Ca-sample}}{{}^{44}Ca/{}_{^{40}Ca-standard}} - 1 \right) * 1000 \qquad \text{(Eq1)}$$

There are three reference scales ('standard' in Eq 1) that have been used throughout the calcium isotope community: seawater (SW), a carbonate standard (915A), and bulk silicate earth (BSE). Each has their advantages and limitations. The carbonate reference scale, 915A, is the most commonly used, suffers from lack of availability for use in many labs as it is no longer commercially available. The BSE standard similarly suffers from the fact that silicate earth varies in its δ^{44}Ca, and some have argued that seawater may vary in a similar manner, making an international agreement on the value of the reference ^{44}Ca/^{40}Ca to use elusive (Kang et al., 2017; Chakrabarti et al., 2018). It has become common practice to report calcium isotope data versus all three reference scales for comparison among various studies and approaches.

The use of δ^{44}Ca to reconstruct the calcium cycle, and by proxy the carbon cycle, over geological time has been challenging. The δ^{44}Ca of all minerals precipitating in the ocean is lower than the δ^{44}Ca of the ocean, that is minerals precipitating take in more of the ^{40}Ca isotope, leaving ^{44}Ca behind (Fantle and DePaolo, 2005, 2007; Kasemann et al., 2005, 2014; Nielsen et al., 2012). This kinetic isotope effect varies in its magnitude, depending largely on the rate of precipitation of the mineral in question and the mineral, or polymorph of calcium carbonate, that is precipitating (Gussone et al., 2003; Tang et al., 2008; Blättler et al., 2012). If you measure only one type of calcium-bearing mineral over time, then any change in the δ^{44}Ca of this mineral could reflect either a change in the δ^{44}Ca of the ocean or a change in the nature and conditions of precipitation of this mineral over Earth history, influencing the calcium isotope fractionation on mineral precipitation. This is further complicated by the fact that many calcium carbonate minerals dissolve, precipitate, and recrystallise during sedimentary diagenesis. This recrystallisation can shift the δ^{44}Ca of the mineral, and not always in the same direction depending on the degree of fluid-buffered versus sediment-

buffered (or open-system versus closed-system) conditions (Fantle and DePaolo, 2005, 2007; Fantle, 2015; Higgins et al., 2018; Ahm et al., 2019).

This problem has been largely circumvented by measuring calcium isotopes in a single mineral, often a biomineral, thus avoiding measurements of bulk carbonate sediments, which may record a range of different primary carbonate mineralogies and where the nature of diagenesis may be difficult to disentangle (Higgins et al., 2018; Ahm et al., 2019; Tostevin et al., this issue). Many studies have explored the calcium isotope fractionation associated with biogenic carbonate mineral precipitation, including corals (Gothmann et al., 2016), foraminifera (Heuser et al., 2005; Hippler et al., 2006; Sime et al., 2007), brachiopods (Farkaš et al., 2007b; Brazier et al., 2015), belemnites (Farkaš et al., 2007a,b; Blättler et al., 2012), and rudists (Immenhauser, 2005). When these records show long-term temporal changes in the calcium isotope composition of the single biomineral, the conclusion is that either the calcium isotopic composition of the ocean has changed (Blättler et al., 2012) or that the calcium isotope fractionation factor on biomineral precipitation has changed (Gothmann et al., 2016).

In theory, if one biomineral is measured, and the calcium isotope fractionation factor for that mineral is known, then a reasonable estimate of seawater $\delta^{44}Ca$ could be made (Blättler et al., 2012). Although seawater calcium should have a single $\delta^{44}Ca$, as calcium is homogenized in the ocean and has a long residence time, the seawater $\delta^{44}Ca$ as reconstructed from single biominerals and calcium-in-barite, over the Phanerozoic, has significant scatter (Figure 1). This range in the $\delta^{44}Ca$ at any given time point has been attributed to difference in the calcium-isotope fractionation factor during mineral precipitation or stabilisation, which has been attributed, at times, to local temperature variability (Tang et al., 2008), changes in the original carbonate-mineral polymorph that precipitated (Gussone et al., 2005), varying rates of carbonate mineral precipitation (DePaolo, 2011), and varying degrees of recrystallization during diagenesis (Higgins et al., 2018). Additionally, all of these biomineral-based proxies for the calcium cycle rely on "bootstrapping" the record to more recent, better characterized species.

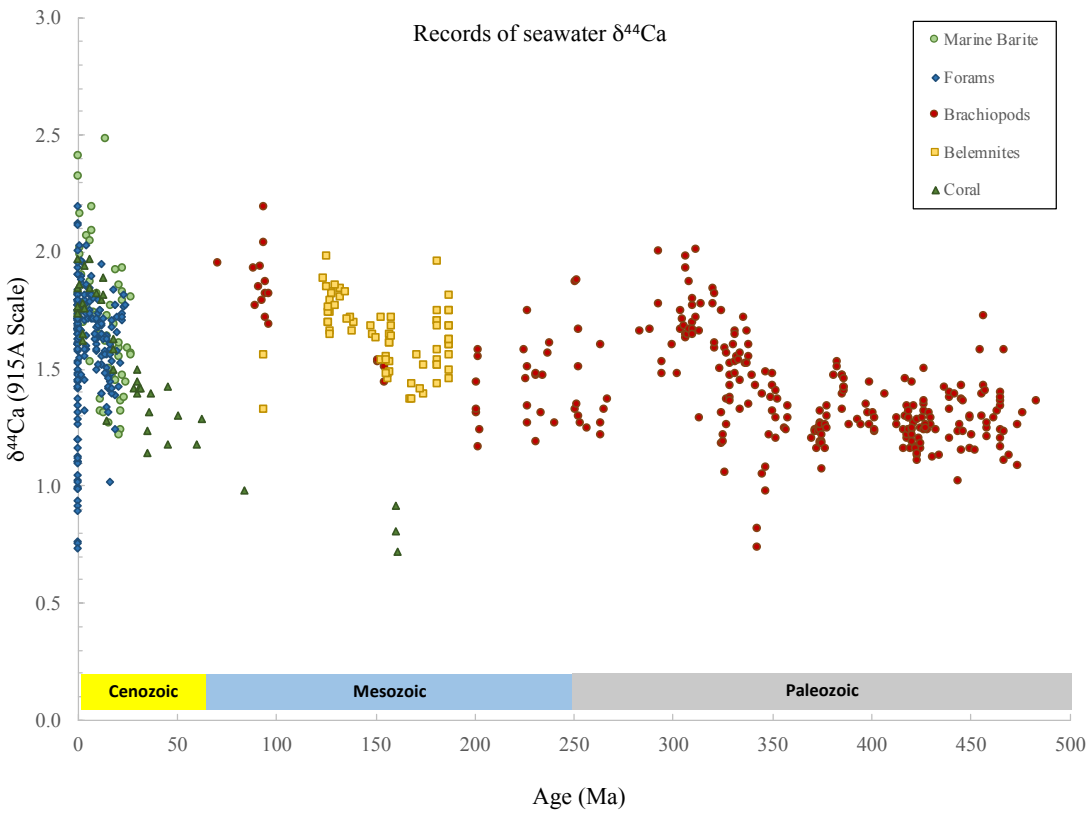

Figure 1. Compiled record of calcium isotopes in biogenic carbonate and marine barite. The raw measurements have been corrected using the 'known' calcium isotope fractionation factors for each biomineral, listed in Table 4, to yield what is thought to be paleo-seawater $\delta^{44}Ca$, allowing the records to be compared to one another as each biomineral has a different calcium isotope fractionation factor. Records include marine barite (purple circles, Griffith et al., 2008); forams (yellow diamonds, Heuser et al., 2005; Hippler et al., 2006; Nägler et al., 2000; Sime et al., 2007), brachiopods (light blue circles, Farkaš et al., 2007a) belemnites (green squares, Blättler et al., 2012; Farkaš et al., 2007a,b), and coral (red triangles, Gothmann et al., 2016). Measurement error, as reported, is typically ~0.1‰ (2σ). Exact uncertainties as reported in the original publications are shown in Figure 2.

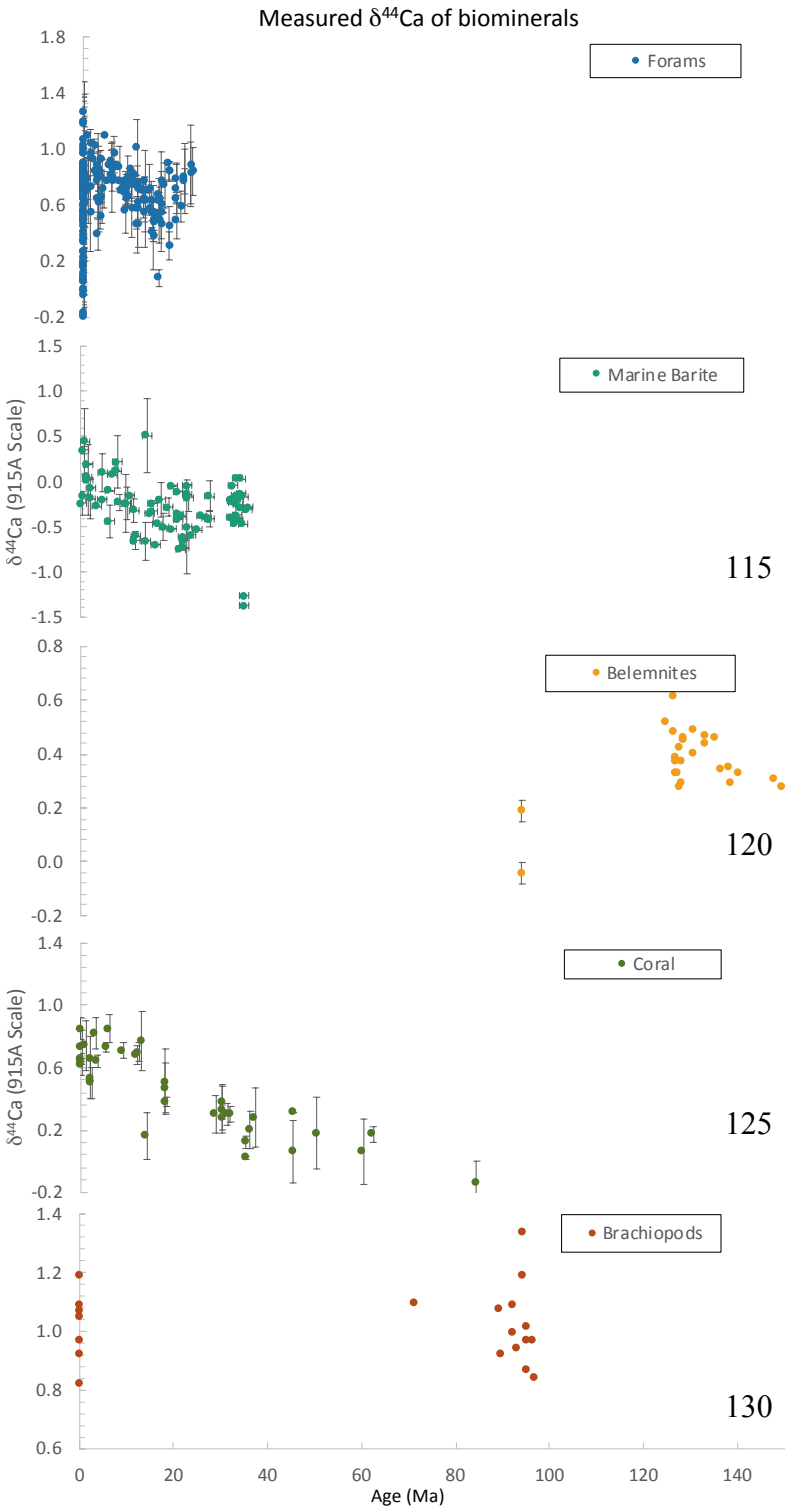

Figure 2. Individual $\delta^{44}Ca$ records for various minerals shown in composite in Figure 1, here not corrected for calcium isotope fractionation (i.e. raw data, on the 915A reference scale). Here, only the last 140 Million years are plotted. Error bars represent reported 2SD error if available.

What is apparent from the various records of $\delta^{44}Ca$ over the Phanerozoic is that there is some broad shape or curvature to the record (Figure 1, 2). In the calcium isotope fractionation-corrected compilation of biominerals in Figure 1, there is an increase in the reconstructed seawater $\delta^{44}Ca$ from the Mesozoic to today. When these corrections are removed and each biomineral is considered independently, this increase in $\delta^{44}Ca$ becomes even more apparent (Figure 2). This increase in $\delta^{44}Ca$ has been seen in other calcium-bearing records not presented here such as phosphates (Schmitt et al., 2003; Soudry et al., 2004, 2006) and evaporite minerals (Blättler and Higgins, 2014). The ambiguity associated with the calcium isotopic fractionation factors of such a range of minerals necessarily makes absolute comparisons challenging. However, the fact that raw comparisons show similar temporal trends (Figure 2) suggests that there is a signal within

these datasets, that each mineral is responding to a similar change possibly in the $\delta^{44}Ca$ of the ocean. It remains an open question what the drivers of a long-term evolution of the $\delta^{44}Ca$ of the ocean might be.

We add to this discussion the analysis of the $\delta^{44}Ca$ of carbonate hardground cements as a further calcium-bearing mineral carrier that we have analysed from nine time periods over the course of the Phanerozoic. Carbonate hardground cements allow for the constraint of some of the variables plaguing other biogenic carbonate minerals records, including the potential skewing of the record given the high degree of biological control exerted by some organisms in making their calcium carbonate skeletons (Blättler et al., 2012, Gothmann et al., 2016). Carbonate hardgrounds are rocks that have rapidly lithified at the sediment/water interface, resulting from a combination of high carbonate saturation state (Rameil et al., 2012; Christ et al., 2015), low sediment accumulation rates (Shinn, 1969; Kennedy and Garrison, 1975), or elevated fluid flow through the subsurface promoting rapid precipitation (Dravis, 1979, Lighty, 1985). The timescale for lithification is variable, though short on a geologic time scale (10's to 1000's years, Christ at al., 2015). Forming at shallow water depths, carbonate hardgrounds are found in warm environments in the modern ocean, such as Pacific atolls (Carpenter et al., 1991), the Arabian Gulf (Khalaf et al., 1987), and the Caribbean (Malone et al., 2001). When sea level falls, carbonate hardgrounds may be subject to meteoric water influence. They are often identified in the geological record from the subsequent boring and encrustation of marine organisms into the lithified rock and their abundance is clustered in the Mesozoic and early Paleozoic (Christ et al., 2015).

In theory, carbonate hardground cements should precipitate at the sediment-water interface and the assumption is that the fluid should be minimally evolved from seawater (Christ et al., 2015). However, pore fluids evolve rapidly in their chemical composition from the sediment-water interface and the $\delta^{44}Ca$ can be particularly variable, given how much more calcium is in the mineral phase relative to the fluid phase (therefore small changes in mineral dissolution and precipitation can greatly impact the $\delta^{44}Ca$ of the pore fluid) (Fantle and DePaolo, 2007; Fantle, 2015). As carbonate hardground cements are effectively inorganic carbonate precipitates that are rapid on geological timescales, they may preserve a seawater signal better than biominerals or other calcium-bearing phases that are subject to varying vital effects or unclear timing of precipitation. Our results will be compared to other existing

records and considered in the context of seawater, porewater, and the carbon cycle evolution over the Phanerozoic.

Methods

Samples from carbonate hardgrounds were obtained from the collections of the London Museum of Natural History, Wooster University, the University of Colorado, Eötvös Loránd University, University of Saskatchewan, and the University of Cambridge. Samples are from the modern, Holocene, Cretaceous, Jurassic, Triassic, Permian, Carboniferous, Ordovician, and Cambrian. These samples were selected based on evidence of early lithification at the sediment/water interface through the presence of marine boring and encrusting organisms. All samples are thought to be either primary or minimally altered calcite. This presumption is based off of both diagenetic and petrographic considerations. For more uniform comparison, any aragonite or previously aragonite cements were visually identified through botryoidal or needle crystal morphology and excluded. Additionally, geochemical evidence of primary or altered aragonite, through low magnesium concentrations or evidence of alternation, resulted in sample exclusion. These samples have been previously analysed for composition and diagenetic alteration using magnesium, strontium, and manganese concentrations, REE, $\delta^{18}O$, $\delta^{13}C$, and $^{87}Sr/^{86}Sr$ ratios (Erhardt et al., in review). Table 1 summarizes the ages and depositional environments of these samples.

Age (Ma)	Stage	Period	Location	Reference	Depositional Environment	Cement type
0	Modern	Neogene	Enewetak Atoll, Marshalls Islands	Carpenter et al., 1991	Shallow water modern Atoll, classic beachrock	Carbonate reef grainstone- fibrous high Mg calcite cement
66	Maastrichtian 1	Cretaceous	Meerssen Member, the Netherlands	van der Ham et al., 2007	From the type section for the Mastrictian. Seagrass present	Bladed low-Mg calcite with blocky pore-filling calcite
66-72	Maastrichtian 2	Cretaceous	Qishn Formation, Oman	Immenhauser et al., 2004	Shallow-water cycle tops, likely intertidal	Microcrystalline calcite
100	Cenomanian	Cretaceous	Upper Greensands, Devon, UK	Gallois, 2005	Subtidal	Microcrystalline calcite
168-170	Bajocian	Jurassic	Tölgyhát Limestone, Gerecse Mts. Of Hungary	Császár et al., 2012	Deepwater sediment, pelagic 'red' limestone	Microcrystalline early calcite with blocky pore-filling calcite
331-347	Visean	Carboniferous	Eskett Limestones, England	Dean et al., 2011	From a cycle top - often calcrete (subaerially exposed)	Platform carbonate- Radiaxial fibrous calcite, secondary blocky pore filling calcite cement
461-468	Dariwillian	Ordovician	Kanosh Formation, Utah	McDowell, 1986	Intertidal and subtidal carbonate sedimentation	Fossiliferous micrite-microcrystalline calcite cement
485-497	Furongian	Cambrian 1	Furongian, Banff National Park	Westrop, 1989	Subtidal, storm dominated shelf	Microcrystalline and drusy calcite
495-505	Drumian	Cambrian 2	Marjuman, Banff National Park	Aitken, 1979	Peritidal	Microcrystaline calcite

190 Table 1- Samples Used in this Study

One key objective was to isolate cements from the primary biominerals that make up the carbonate hardground. Early cements were identified by their distinct chemical composition, including concentrations of magnesium, calcium, strontium, manganese, and rare earth elements (Erhardt et al., in review) from both the primary clasts and any interior-pore precipitation. Samples for calcium isotope analysis were collected using a tungsten needle with 1μm point under an optical microscope or microdrilled, attempting to collect only the authigenic carbonate phase (Dickson et al., 2008). Approximately ~1-2 mg of sample was collected to support multiple geochemical analysis, though only 10 μg was needed for each calcium analysis. The procedural blank from sample dissolution and separation on the Dionex ICS5000+ HPIC, as determined independently by ICP-OES, is 96 ng of calcium when 7 ml of eluent was collected from the Dionex. During the collection of 4.4 mg of calcium using the Dionex, this represents ~2% of the collected calcium.

These carbonate samples were dissolved in distilled 2% nitric acid, spiked with ^{42}Ca and ^{48}Ca, and the calcium was isolated from other cations using a Thermo Fisher Scientific Dionex ICS5000+ HPIC following the methods of Bradbury and Turchyn (2018). This sample, approximately 4 μg of calcium, was loaded onto rhenium filaments with phosphoric acid as an activator. The calcium isotope ratios were analyzed on a Thermo Fisher Scientific Triton Plus Multicollector Thermal Ionization Mass Spectrometer (TIMS) at the University of Cambridge. The NIST carbonate standard 915B was analyzed every 4-5 samples. Based on the long-term reproducibility of the 915B standard, an error of 0.09‰ (2σ) was assigned to all analyses.

When we present previously published data, the conversion between $\delta^{44/42}Ca$ and $\delta^{44/40}Ca$ was made using the conversion in Sime et al. (2005) (Equation 2) . Results used from Blättler et al. (2012) were converted to account for differences from precipitation temperature. Given the overall small magnitude of that conversion relative to the magnitude of change in $\delta^{44}Ca$ observed in this study, further temperature conversions were not applied other samples in this study.

Equation 2:

$$\delta^{44/42}Ca = \left(\frac{\frac{1}{m_{42}} - \frac{1}{m_{44}}}{\frac{1}{m_{40}} - \frac{1}{m_{44}}}\right) * \delta^{44/40}Ca = 0.476\,\delta^{44/40}Ca$$

Results

The δ^{44}Ca of carbonate hardground cements ranges from 0.47 to 1.53 (‰ 915A) with one outlier from the late Cretaceous at +1.83 (‰ versus 915A – Table 1, Figure 3). Within any time interval sampled, the range in the δ^{44}Ca of the carbonate cement is relatively narrow, between 0.05‰ and 0.56‰ (among data points of the same time interval), disregarding the outlier from the late Cretaceous. Within each time period we report multiple analyses of chronically adjacent hardgrounds, along with the sampling of both the earliest and likely secondary cements when this fine degree of sampling was possible. All δ^{44}Ca data from our carbonate hardground cements lie below the reconstructed δ^{44}Ca for seawater over the Phanerozoic (Figure 3), as expected during carbonate mineral precipitation where the ^{40}Ca is preferentially taken into the carbonate mineral lattice.

Age		Location	□^{44}Ca (‰ BSE)	□^{44}Ca (‰ SW)	□^{44}Ca (‰ 915A)
0	Modern	Enewetak Atoll, Marshalls Islands	0.42	-0.52	1.42
0	Modern	Enewetak Atoll, Marshalls Islands	0.43	-0.51	1.43
0	Modern	Enewetak Atoll, Marshalls Islands	0.53	-0.41	1.53
0	Modern	Enewetak Atoll, Marshalls Islands	0.46	-0.48	1.46
66	Maastrichtian 1	Meerssen Member, the Netherlands	0.23	-0.71	1.23
66	Maastrichtian 1	Meerssen Member, the Netherlands	0.34	-0.60	1.34
66-72	Maastrichtian 2	Quishn Formation, Oman	-0.03	-0.97	0.97
66-72	Maastrichtian 2	Quishn Formation, Oman	0.02	-0.92	1.02
66-72	Maastrichtian 2	Quishn Formation, Oman	0.13	-0.81	1.13
66-72	Maastrichtian 2	Quishn Formation, Oman	0.21	-0.73	1.21
66-72	Maastrichtian 2	Quishn Formation, Oman	0.83	-0.11	1.83
100	Cenomanian	Upper Greensands, Dunscome Cliff, Devon, UK	0.07	-0.87	1.07
100	Cenomanian	Upper Greensands, Dunscome Cliff, Devon, UK	0.11	-0.83	1.11
100	Cenomanian	Upper Greensands, Dunscome Cliff, Devon, UK	0.12	-0.82	1.12
168-170	Jurassic	Tölgyhát Limestone, Gerecse Mts. Of Hungary- Composite	-0.19	-1.13	0.81
168-170	Jurassic	Gerecse Mts. Of Hungary- Composite	-0.20	-1.14	0.80
168-170	Jurassic	Geresce Sequence 1- earliest cement	-0.53	-1.47	0.47
168-170	Jurassic	Geresce Seq. 1- intermediate cement	-0.42	-1.36	0.58
168-170	Jurassic	Geresce Sequence 1- later cement	-0.05	-0.99	0.95
168-170	Jurassic	Geresce Sequence 2- earliest cement	-0.46	-1.40	0.54
168-170	Jurassic	Geresce Sequence 2- later cement	0.03	-0.91	1.03
331-347	Mississipian	Sixth/Seventh Limestones, Eskett Limestones, England	-0.38	-1.32	0.62
331-347	Mississipian	Sixth/Seventh Limestones, Eskett Limestones, England	-0.35	-1.29	0.65
331-347	Mississipian	Sixth/Seventh Limestones, Eskett Limestones, England	-0.32	-1.26	0.68
461-468	Ordovician	Kanosh Formation, Utah	-0.20	-1.14	0.80
461-468	Ordovician	Kanosh Formation, Utah	-0.15	-1.09	0.85
485-497	Cambrian 1	Furongian, Banff National Park	-0.44	-1.38	0.56
495-505	Cambrian 2	Marjuman, Banff National Park	-0.07	-1.01	0.93
495-505	Cambrian 2	Marjuman, Banff National Park	-0.07	-1.01	0.93
495-505	Cambrian 2	Marjuman, Banff National Park	-0.04	-0.98	0.96
495-505	Cambrian 2	Marjuman, Banff National Park	0.03	-0.91	1.03

Table 2 - Our data, including the age, Period or Epoch, location where the sample comes from, its calcium isotope composition versus bulk silicate earth, seawater, and vs. 915A.

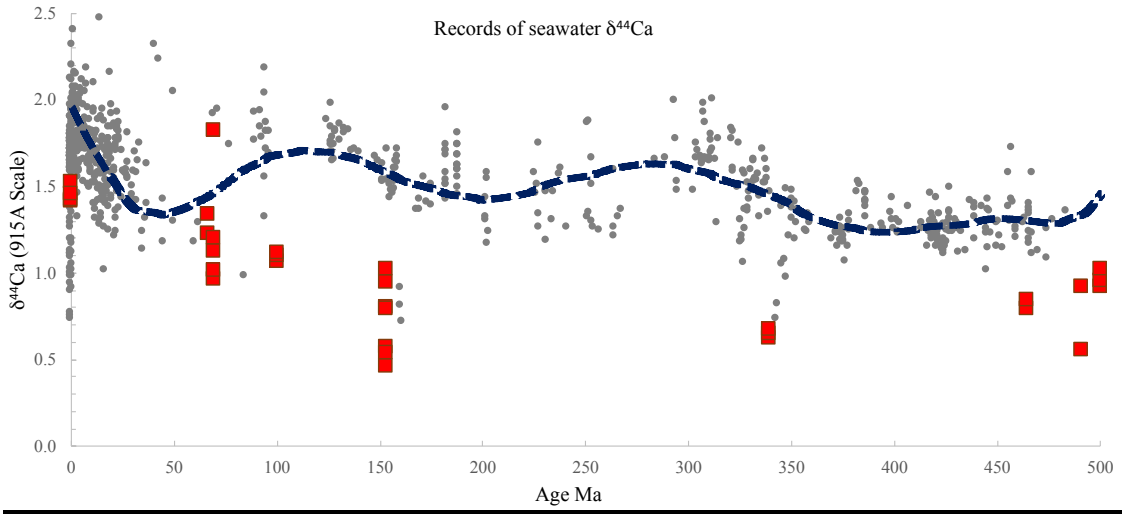

Figure 3. Results from this study (red squares) of $\delta^{44}Ca$ in carbonate hardground cements. The grey dots represent the complied existing data as seawater (see also Figure 1), with the dark dashed line representing the average fit through those results, as a 'best estimate' curve of the $\delta^{44}Ca$ of the ocean over time from which the carbonate hardground cements precipitate. Measurement error for our samples is ± 0.09‰ (2σ).

Discussion

Range in the $\delta^{44}Ca$ of the carbonate hardground cements

At any given point in time, we observe a range of $\delta^{44}Ca$ measured in the carbonate hardground cement samples of between 0.54‰ and 1.03‰ (Table 2, Figure 3). In theory, if the carbonate hardground cements were precipitating in a fully closed system, then the initial carbonate precipitate would be offset from the $\delta^{44}Ca$ of the pore fluid by some amount determined by the polymorph of carbonate mineral precipitated and the rate of mineral precipitation. This removal of ^{40}Ca would leave ^{44}Ca behind in the pore fluid, and the next carbonate mineral to precipitate would derive from this isotopically evolved fluid, differing in its $\delta^{44}Ca$ from the initial carbonate mineral precipitate. In modern environments where carbonate minerals are precipitating, this distillation (i.e. Rayleigh fractionation) of calcium isotopes has been seen in the sedimentary pore fluids, and has been used to reconstruct the rate of carbonate mineral precipitation and its calcium isotope fractionation (Teichert et al., 2009; Bradbury and Turchyn, 2018). During the subsequent recrystallization of carbonate minerals, the pore fluids evolve to a lower $\delta^{44}Ca$, reflecting the addition of ^{40}Ca-rich from carbonate mineral phases (it is thought that there is no calcium isotope fractionation on

dissolution) (Fantle and DePaolo, 2005, 2007; Fantle, 2015). The range of $\delta^{44}Ca$ that has been measured in modern sedimentary pore fluids is approximately 2‰ due to this range of processes (Fantle and DePaolo 2005, 2007; Turchyn and DePaolo, 2011; Fantle, 2015; Bradbury and Turchyn, 2018).

In the case of carbonate hardground cements, we expect the pore fluids to be affected less by recrystallization or mineral dissolution lowering the $\delta^{44}Ca$ of the pore fluid, and more by the amount of carbonate cement precipitation and the degree of open-versus-closed system conditions during cement formation. This is because of the rapid nature of carbonate hardground cement precipitation near to the sediment-water interface. If the system is 'closed' and carbonate mineral precipitation is occurring, we should see the isotopic distillation discussed above; this would be reflected in an increase in the $\delta^{44}Ca$ across the cement. However, if the system is more 'open' – largely to exchange with seawater or other fluids, this distillation may not be seen, and a more constant $\delta^{44}Ca$ found in the precipitating cements.

We see two examples of closed-system carbonate mineral precipitation in our carbonate hardground cements. In one Jurassic sample we were able to identify and sample multiple cement phases using a tungsten needle. This sample shows three distinct phases of precipitation, transitioning from a micrite to blocky calcite phases. There is an increase in the $\delta^{44}Ca$ of the cement with growth (Figure 4). In this case, the early phase may be a rock-buffered pore fluid (i.e. Pruss et al., 2018) with the following cements from burial or later diagenetic processes. In theory, as the cement grows onto the previously precipitated carbonate mineral, the initial mineral precipitate is not isotopically reset.

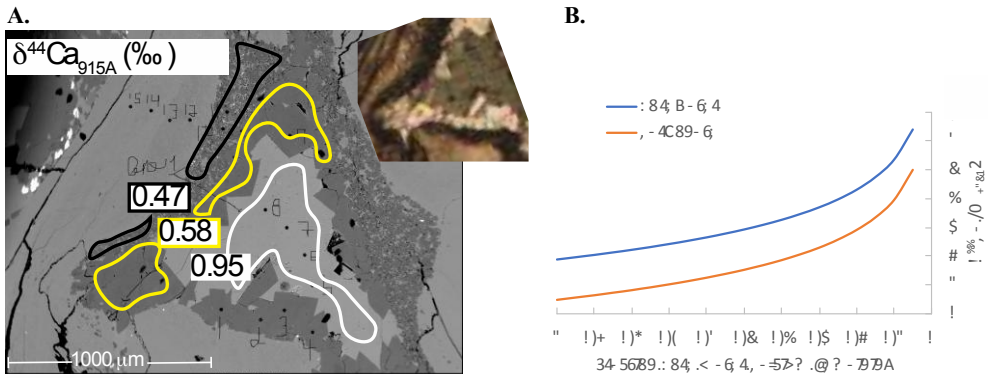

Figure 4. A) Three layers of the Jurassic carbonate hardground cement show an increase in the $\delta^{44}Ca$ of subsequent layers of carbonate precipitation with increasing $\delta^{44}Ca$. The inset picture shows the optical image of this sample. B) Rayleigh fractionation of porewater and carbonate during simple carbonate precipitation in a closed system with a constant calcium isotope fractionation factor of $\alpha = 0.9985$ (DePaolo, 2011).

If we assume both the initial $\delta^{44}Ca$ of the fluid, a constant calcium isotope fractionation factor, and closed system precipitation, the $\delta^{44}Ca$ of the cement could be used to track the fraction of calcium remaining in the porewater during cement precipitation (Figure 4B). However, this would assume that we know both what the $\delta^{44}Ca$ of the initial pore fluid was at this time, the calcium isotope fractionation on mineral precipitation and, more critically, that there was no local mineral dissolution (or recrystallisation). All three of these assumptions are not well constrained. In marine sediments dominated by sedimentary carbonate mineral precipitation, although carbonate mineral precipitation exceeds the rate of dissolution by as much as 10 or 20 times, there is still some mineral dissolution as suggested by pore fluid models (Fantle and DePaolo, 2005, 2007; Fantle, 2015; Huber et al., 2017; Bradbury and Turchyn, 2018).

We can make a simple assumption that in modern sedimentary pore fluids where there is active carbonate precipitation occurring, the $\delta^{44}Ca$ of the pore fluid is either equal to or higher than seawater (but critically not less than). This is consistent with modern sedimentary pore fluids in sediment with active sedimentary carbonate precipitation. While there is no current data of pore water $\delta^{44}Ca$ in the upper centimeters of the sediment column where hardgrounds form, the initial pore fluid $\delta^{44}Ca$ that has been reported at 3 or 5 meters below the surface is often at or higher than seawater $\delta^{44}Ca$ (Teichert et al., 2007; Turchyn and DePaolo 2011; Bradbury and Turchyn, 2018) with the exception of samples from Site 807A

(Fantle and DePaolo 2007). This means that in any given time interval, the lowest $\delta^{44}Ca$ we measure in the carbonate hardground cement may represent the earliest precipitate, and therefore the one that precipitated from the least evolved pore fluid, closest to seawater $\delta^{44}Ca$. Making this assumption gives an estimate of the calcium isotope fractionation factor on carbonate hardground cement precipitation and a bound on the trajectory of changes in the $\delta^{44}Ca$ of the fluid over time.

We use this assumption to estimate the calcium isotope fractionation factor for the various carbonate hardground cements (Table 3), which averages -0.57 ± 0.27‰ for the nine time intervals studied. There is a range in calcium isotope fractionation for the carbonate hardground cements, with the lowest calcium isotope fractionation in the Cretaceous carbonate hardground cement (-0.22‰) and the highest in the Jurassic (-1.11‰). There are several reasons why these numbers should be taken as very rough estimates rather than firm calcium isotope fractionation factors. For example, the reconstruction of seawater $\delta^{44}Ca$ (Figure 3) is highly uncertain, and furthermore it is likely that the initial fluids from which the carbonate hardground cements precipitated are evolved in some way from any paleo-seawater $\delta^{44}Ca$. Furthermore, given the physical difficulty of only sampling the cement, it is probable that some of the host carbonate biominerals were included in our analysis. Hence, the measured $\delta^{44}Ca$ may not only record cement from pore fluids. Accidental sampling of the biomineral with the cement would skew our data lower in its $\delta^{44}Ca$ on the whole, and thus the calculated calcium isotope fractionation during carbonate hardground cement precipitation (Table 3) would be larger than in reality.

With these caveats on our calculated calcium isotope fractionation factor during carbonate hardground cement formation, we can compare our average (-0.57±0.27‰) to the calcium isotope fractionation factor for other calcium-bearing carbonate minerals. We note that in general the calcium isotope fractionation for inorganic carbonate precipitates is less than for biogenically precipitated minerals (Table 4), and our carbonate hardground cement data has a similar calcium isotope fractionation as inorganic calcite. It is also consistent with the estimated calcium isotope fractionation calculated at the 'kinetic limit' for inorganic carbonate mineral precipitates (Nielsen et al., 2012). We suggest that the calcium isotope fractionation on carbonate hardground cement precipitation is kinetically controlled and not growing at equilibrium with the pore fluids, and unlikely to be recrystallised in fluid-buffered conditions.

Age of hardground		Lowest cement $\delta^{44}Ca$ (‰ 915A)	Interpolated seawater $\delta^{44}Ca$ (‰ 915A)	Calcium isotope fractionation factor (‰)
0	Modern	1.42	1.84	- 0.42
66	Maastrichtian 1	1.23	1.45	- 0.22
66-72	Maastrichtian 2	0.97	1.48	- 0.51
100	Cenomanian	1.07	1.69	- 0.62
168-170	Jurassic	0.47	1.58	- 1.11
33`-347	Carboniferous	0.62	1.44	- 0.82
461-468	Ordovician	0.8	1.29	- 0.49
485-497	Cambrian 1	0.56	1.24	- 0.68
495-505	Cambrian 2	0.93	1.24	- 0.31
Average				**-0.57 ± 0.27‰**

Table 3. Lowest measured $\delta^{44}Ca$ in the carbonate hardground cement, the interpolated seawater $\delta^{44}Ca$, and the calculated calcium isotope fractionation factor during cement precipitation from each time period studied.

We compare our hardground cements with other Phanerozoic carbonate cements. Previously published $\delta^{44}Ca$ of carbonate cements aren't from hardgrounds and therefore may have more ambiguity regarding the timing of precipitation, however they serve as a check for our calcium isotope fractionation factor. Steuber and Buhl (2006) measured Cenomanian "diagenetic calcite" with an average $\delta^{44}Ca$ of 1.1 +/- 0.05‰ 2SD (converted to $\delta^{44}Ca$ on the 915A reference scale), which is identical to our Cenomanian sample of 1.1 +/- 0.06‰ 2SD. Additionally, the Steuber and Buhl (2006) $\delta^{44}Ca$ for Carboniferous cement was 1.14 +/- 0.15‰ 2SD, which is higher than our Mississippian $\delta^{44}Ca$ of 0.62 +/- 0.05‰ 2SD. Our Mississippian carbonate hardground cement $\delta^{44}Ca$ are among the lowest $\delta^{44}Ca$ that we have measured (Figure 3). Other studies have analysed calcite cements filling voids in Cretaceous (Toronian) ocean basalts at 1.3 – 1.5‰ (Weinzierl et al., 2018) and Ediacaran age cements that were originally aragonite at ~0.6‰ (Pruss et al., 2018). These $\delta^{44}Ca$ for other carbonate

Carbonate Phase/ Seawater Proxy	Approx. calcium isotope fractionation from seawater (‰)	Source
Inorganic calcite	-0.57 +/- 0.27	This Study

	-0.4 to -1.6 dependent on rate	Tang et al., 2008 (laboratory study)
	-0.6 to -0.7	Nielsen et al., 2012 (modelled result)
	-0.6 to -0.8	Marriott et al., 2004 (laboratory study)
Brachiopod	-0.85	Farkaš et al., 2007a
Forams	-0.94	Heuser et al., 2005
	-1.4 to -1.1	Sime et al., 2005
	-1.2 to -0.8 (Orbulina universa)	Gussone et al. 2003
Coral	-1.12 (modern seawater) $\Delta_{(Coral-SW)}$ = -0.06 ± 0.01*[Ca] - 0.6 ±-0.2	Gothmann et al., 2016
	-1.2 at 21° C -1.0 at 29° C	Böhm et al., 2006
Belemnites	-1.40	Farkaš et al., 2007b
Inorganic aragonite	-1.8 at 10°C and -1.5 at 30°C	Gussone et al., 2003
Marine barite	–2.01 +/- 0.15	Griffith et al., 2008

Table 4. Compilation of calcium isotope fractionation from fluid for inorganic and biogenic carbonate minerals from modern seawater.

cements compare favourably with our results for the $\delta^{44}Ca$ of carbonate hardground cements.

This range of calcium isotope fractionation during the precipitation of different biogenic and non-biogenic minerals remains a focus of research (Table 4). The calcium isotope fractionation during carbonate mineral precipitation is largely driven by environmental conditions, such as temperature and ion concentration, that impact the rate of mineral precipitation. The controls on the rate of carbonate mineral precipitation have been investigated in detail by multiple workers and are only briefly summarised here (Lemarchand et al., 2004; Gussone et al., 2005; Tang et al., 2008; DePaolo, 2011). Ultimately the rate of mineral precipitation is related to the concentration of calcium and dissolved inorganic carbon, which determines whether the precipitation is controlled by the concentration of ions at the surface or the need to transport these ions to the surface of the growing mineral

('surface-controlled' versus 'transport-controlled') (DePaolo, 2011). When a carbonate mineral is growing under 'surface-controlled' conditions then it is closer in theory to thermodynamic equilibrium and therefore the calcium isotope fractionation is lower, while in 'transport-controlled' there is a larger calcium isotope fractionation (Fantle and DePaolo, 2007). These scenarios were modelled by DePaolo (2011) to empirically determine the relationship between precipitation rate vs. calcium isotope fractionation. This work was continued in Nielsen et al. (2012) where they developed a model to simultaneously consider both growth rate and calcium isotope fractionation as a function of solution stoichiometry and oversaturation. Overall, they found that the relationship of the concentration of calcium versus carbonate ions influences the calcium isotope fractionation factor; significantly higher concentrations of calcium versus that of carbonate ions drives the system toward isotopic equilibrium (Nielsen et al., 2012). However, increasing supersaturation overall, that is increasing both the concentration of calcium and carbonate ions, drives the system toward kinetic end-members, increasing the precipitation rate and increasing the calcium isotope fractionation factor (Nielsen et al., 2012). Using this model, inorganic carbonate mineral precipitation, particularly calcite, from seawater gave a calcium isotope fractionation factor between -0.6‰ and -0.7‰ (Nielsen et al., 2012), similar to both laboratory studies and our results from inorganic calcite hardground cements.

The rate of carbonate hardground cement precipitation is likely much slower than laboratory experiments, i.e. less than 10^{-9} mol/m^2/s (Tang et al., 2008), and much higher than the rates in deep-sea sediments of ~10^{-17} mol/m^2/s (Fantle and DePaolo, 2007). This is based in the anecdotal evidence of the formation of carbonate hardgrounds over 10's – 100's of years (Christ et al., 2015). This gives support to the idea that the carbonate hardground cements are precipitating near a kinetic limit and the calcium isotope fractionation factor could be similar to laboratory experiments and those predicted from modeling (Nielsen et al., 2012). In contrast, biomineral precipitation dominantly occurs within microenvironments, where locally the saturation state can be greater than surface seawater, which will impact the rate of mineral precipitation (Bentov and Erez, 2005; Sime et al., 2005). As a result, the calcium isotopic fractionation of biogenic minerals from seawater is typically greater than inorganic precipitates and can scale differently with changes in biomineral growth rate (Table 4, Blättler et al., 2012).

Change in the calcium isotope composition of the ocean over time

Our data add to the growing weight of evidence suggesting that the calcium isotopic composition of the ocean can change over geological time. While we can't resolve possible changes in the calcium isotope fractionation factor changing over geological time, we do observe the same increase in the $\delta^{44}Ca$ over the late Mesozoic and Cenozoic that has now been reported for biominerals and calcium-in-barite (Figure 1, 2). Going forward, it will be key to resolve both the magnitude and the timing of this change in seawater $\delta^{44}Ca$. As we better understand the actual calcium isotope fractionation factor during mineral precipitation, and measure a wider range of minerals, we will be able to better tease out the magnitude, timing, and rate of change in the $\delta^{44}Ca$ of seawater.

There are several observations we can make now that will help frame the future research and discussion on this change in seawater $\delta^{44}Ca$. First, it is notable that the change in the $\delta^{44}Ca$ observed in our data and seen in other calcium-bearing mineral proxies is on a longer time scale than one would expect given the short (~0.6-1 Myr) residence time of calcium in the ocean (Fantle and Tipper, 2014). Indeed, during short-term perturbations to the carbon - and linked calcium - cycles, there have been previously reported perturbations to the $\delta^{44}Ca$ that are not fully linked to changes in depositional mineralogy (Payne et al., 2010; Griffith et al., 2015). However, the change observed over the Cenozoic and into the Mesozoic is over closer to 50-60 Million years, much longer than would be expected given the short residence time of marine calcium.

Any driver of an increase in the $\delta^{44}Ca$ of the ocean must either remove more of the ^{40}Ca isotope (or less of the ^{44}Ca isotope) or add more of the ^{44}Ca isotope (or less of the ^{40}Ca isotope). The calcium biogeochemical cycle is dominated by one source (river weathering) and one sink (carbonate mineral deposition), with a smaller contribution from hydrothermal circulation and chemical reaction with clay minerals and the off-axis oceanic crust. Due to the dominance of one source and one sink, it has been thought to be difficult to fundamentally change the $\delta^{44}Ca$ of the ocean, as the $\delta^{44}Ca$ of the source and sink are similar, and fundamentally the surface calcium cycle is dominated by the recycling of carbonate minerals and rocks throughout Earth's surface environments (Blättler et al., 2012; Gothman et al., 2016; Blättler and Higgins, 2017).

One possibility is a change in chemical weathering over the Mesozoic and Cenozoic. As calcium in rivers is dominated by carbonate weathering, which has much more ^{40}Ca in it (rivers have low $\delta^{44}Ca$), a river-driven increase in the $\delta^{44}Ca$ of the ocean would imply a shift to more silicate-sources calcium or a reduction in carbonate weathering (Sime et al., 2007; Griffith et al., 2008.) Driving changes in the $\delta^{44}Ca$ of the ocean by changes in chemical weathering has been previously explored by Fantle and Tipper (2014), where they showed that a switch from rivers weathering 100% carbonate minerals to weathering 100% silicate minerals would only result in a ~0.4‰ shift in marine $\delta^{44}Ca$, making it an ineffective lever to change marine $\delta^{44}Ca$. Tectonic events over the late Mesozoic and Cenozoic, particularly the uplift of the Himalayas (60-40 Ma) and Andes (50-30 Ma), would in theory expose more silicate minerals for chemical weathering increasing the $\delta^{44}Ca$ of riverine calcium. However, the uplift of the Alps, a dominantly carbonate-rock mountain range also occurred over this time interval which might counteract any change in river $\delta^{44}Ca$ from the weathering of silicate terranes. Furthermore, it is unclear whether there is enough calcium in silicate rocks relative to the large amount in carbonate rocks to drastically change the $\delta^{44}Ca$ of the river input.

Another driver of a change in the $\delta^{44}Ca$ of the ocean could be the switch between calcite-dominated and aragonite-dominated oceans (Sime et al., 2007, Farkaš et al. 2007a, Blättler et al., 2012). In the Mesozoic, the dominant carbonate polymorph precipitated was calcite (Stanley and Hardie, 1998), in oceans that had higher overall calcium concentrations and lower magnesium and sulfate concentrations than the modern ocean. In contrast, aragonite is the thermodynamically preferred carbonate polymorph in the modern ocean (Friedman et al., 1965), particularly for marine invertebrates (Zhuravlev and Wood, 2009) and inorganic carbonate minerals (Christ et al., 2015). If all other environmental variables are equal (temperature and rate of mineral precipitation), aragonite has more ^{40}Ca in it, or a larger calcium isotope fractionation factor from seawater than calcite, and has been shown across multiple carbonate-precipitating organisms (~0.6‰ more depleted than calcite – Table 4 – Blättler et al., 2012). In principle, if more carbonate-as-aragonite is removed from the ocean, more ^{40}Ca will be removed as well, driving the $\delta^{44}Ca$ of the ocean to higher, or more ^{44}Ca-enriched values. Large shifts in the abundance of aragonitic vs. calcitic precipitating organisms have been observed throughout the Phanerozoic, that might support this driver of ocean $\delta^{44}Ca$ (Zhuravlev and Wood, 2009). The problem with this explanation is that

carbonate minerals will recrystallise during diagenesis, with the aragonite recrystalising to calcite, which is a more stable carbonate mineral polymorph. In certain unique conditions of carbonate recrystallisation, the aragonite-turned-calcite will retain the lower $\delta^{44}Ca$ from its precipitation, however most of the time the calcite ultimately formed will acquire a new $\delta^{44}Ca$ during recrystallisation and be higher than the initially precipitated aragonite (Higgins et al., 2018; Pruss et al., 2018). Thus it isn't clear that precipitating more carbonate-as-aragonite would ultimately result in removing more ^{40}Ca from the ocean.

However, the $\delta^{44}Ca$ of carbonate minerals deposited in shallow marine environments is fundamentally more ^{44}Ca-enriched, or 'isotopically heavy' than the $\delta^{44}Ca$ of carbonate minerals deposited in deep-marine environments. The reason for this is thought to be that high fluid flow through shallow carbonate platforms and carbonate-rich sediments tends to increase the $\delta^{44}Ca$ of the carbonate minerals towards those in equilibrium with seawater (Fantle and DePaolo 2007; Higgins et al., 2018). Carbonate platforms are fluid-buffered systems, i.e. open systems with sufficient and repeated exposure to the overlying ocean to overprint the initial mineral $\delta^{44}Ca$. While certainly not all shallow marine environments are fluid buffered, shallow marine environments like have greater fluid flow through submarine groundwater discharge, changes in eustatic sea level, evaporation-driven density gradients, etc. (Higgins et al., 2018). This results in carbonate minerals in shallow marine environments that are, on the whole higher, and closer to seawater $\delta^{44}Ca$.

In contrast, the $\delta^{44}Ca$ of carbonate minerals in deep marine environments tend to preserve their original water-column acquired $\delta^{44}Ca$, or at a minimum remain around 1 to 1.4‰ lower than seawater. Fluid flow through deep marine sediments is restricted, partially due to the increased clay compositions of these sediments and lower external fluid-forcing mechanisms; this creates a sediment-buffered system. A shift, therefore, from carbonate mineral burial primarily in shallow, fluid buffered environments, to carbonate mineral burial partitioned between shallow and deep environments could result in preferentially more ^{40}Ca being removed from the ocean, driving the $\delta^{44}Ca$ of the ocean higher.

Exactly such a scenario happened in the middle Mesozoic, with the Marine Mesozoic Revolution (Ridgwell, 2005). The Marine Mesozoic Revolution was the colonising of the open ocean by pelagic calcifying organisms, pushing carbonate mineral production into open

water columns, where before it had been confined to near continental shelf and slope environments. The Marine Mesozoic Revolution has been suggested to have changed the regulation of the carbon cycle (Ridgwell and Zeebe, 2005) by creating a pelagic carbonate sink, which enabled Earth's system to better respond to perturbations to the carbon cycle (Payne et al., 2010). This pelagic carbonate sink would have had more ^{40}Ca in it, and this would have allowed the $\delta^{44}Ca$ of the ocean to increase through the expansion of this deep carbonate sink (initially suggested in Blättler et al., 2012). Future work focusing on this interval with the calcium isotopic composition of the ocean in mind would both verify the dynamics of this event and constrain the sensitivity of the ocean calcium reservoir to shifts in sink locations, highlighting the applicability of the calcium isotope proxy.

Conclusions

We have measured the $\delta^{44}Ca$ in carbonate hardground cements in samples spanning the Phanerozoic. When compared to the existing datasets of biogenic minerals, similar trends of lower $\delta^{44}Ca$ further back in time are observed. It appears increasingly likely that independent coral, foraminifera, marine barite, and inorganic carbonate precipitates are reflecting changes in the isotopic composition of the calcium ocean reservoir. The offset between a reconstructed seawater $\delta^{44}Ca$ and the lowest $\delta^{44}Ca$ in the carbonate hardground cements is 0.57±0.27‰, consistent with the calcium isotope fractionation for inorganic carbonate precipitates in laboratory studies (Tang et al., 2008) and predicted from models (Nielson et al., 2012). Looking forward, the analysis of additional carbonate hardground cements may help constrain both pore water dynamics and seawater calcium isotopic composition during times of change in the Phanerozoic. Future directions include the modelling of the amount of ^{44}Ca that would need to be sequestered over time in fluid vs sediment buffered systems to change the ocean $\delta^{44}Ca$ and higher resolution records involving single biominerals to better constrain the timing and nature of changes in marine $\delta^{44}Ca$. Carbonate hardground cements offer a promising new avenue for studying earliest marine diagenesis and the evolution of seawater chemistry.

Acknowledgements

We gratefully thank Paul Taylor, Mark Wilson, David Budd, Orsolya Győri, Brian Pratt and Stephen Lokier for providing samples for this study. We are thankful to the two anonymous reviewers, along with the editor, who greatly improved the manuscript. Funding for this

project was provided by the Canadian Institute for Advanced Research (CIFAR) to AME and ERC StG Grant 307582 (CARBONSINK) to AVT.

References

Ahm, A.S.C., Maloof, A.C., Macdonald, F.A., Hoffman, P.F., Bjerrum, C.J., Bold, U., Rose, C.V., Strauss, J.V., Higgins, J.A., 2019. An early diagenetic deglacial origin for basal Ediacaran "cap dolostones." Earth Planet. Sci. Lett., 506, 292-307.

Bentov S., Erez J., 2005. Novel observations on biomineralization processes in foraminifera and implications for Mg/Ca ratio in the shells. Geology, 33, 841–844.

Blättler, C.L., Henderson, G.M., Jenkyns, H.C., 2012. Explaining the Phanerozoic Ca isotope history of seawater. Geology, 40, 843-846.

Blättler, C.L., Higgins, J.A., 2014. Calcium isotopes in evaporites record variations in Phanerozoic seawater SO_4 and Ca. Geology, 42, 711-714.

Blättler, C.L., Higgins, J.A., 2017. Testing Urey's carbonate–silicate cycle using the calcium isotopic composition of sedimentary carbonates. Earth Planet. Sci. Lett., 479, 241-251.

Böhm, F., Gussone, N., Eisenhauer, A., Dullo, W.C., Reynaud, S., Paytan, A., 2006. Calcium isotope fractionation in modern scleractinian corals. Geochim. Cosmochim. Acta 70, 4452–4462.

Bradbury, H.J, Turchyn, A.V., 2018. Calcium isotope fractionation in sedimentary pore fluids from ODP Leg 175: Resolving carbonate recrystallization. Geochim. Cosmochim. Acta, 236, 121–139.

Brazier, J.-M., Suan, G., Tacail, T., Simon, L., Martin, J. E., Mattioli, E., Balter, V., 2015. Calcium isotope evidence for dramatic increase of continental weathering during the Toarcian oceanic anoxic event (Early Jurassic). Earth Planet. Sci. Lett. 411, 164–176.

Carpenter, S.J., Lohmann, K.C., Holden, P., Walter, L.M., Huston, T.J., Halliday, A.N., 1991. $\delta^{18}O$ values, $^{87}Sr/^{86}Sr$ and Sr/Mg ratios of Late Devonian abiotic marine calcite: implications for the composition of ancient seawater. Geochim. Cosmochim. Acta 55, 1991–2010.

Chakrabarti, R., Acharya, S.S., Mondal, S., 2018. Large stable Ca isotopic (δ44/40 Ca) variation in open ocean samples from the Bay of Bengal. Goldschmidt Abstracts, 359.

Christ, N., Immenhauser, A., Amour, F., Mutti, M., Preston, R., Whitaker, F.F., Peterhänsel, A., Egenhoff, S.O., Dunn, P.A., Agar, S.M., 2012. Triassic latemar cycle tops—subaerial exposure of platform carbonates under tropical arid climate. Sediment. Geol. 265-266, 1–29.

Christ, N., Immenauser, A., Wood, R.A., Darwich, K., Niedermayr, A., 2015. Petrography and environmental controls on the formation of Phanerozoic marine carbonate hardgrounds. Earth-Science Reviews, 15, 176–226.

Császár, G., Haas, J.,Sztanó, O., Szinger, B., 2012. From Late Triassic passive to Early Cretaceous active continental margin of dominantly carbonate sediments in the Transdanubian Range, Western Tethys. Journal of Alpine Geology, 55.

De La Rocha, C.L., DePaolo, D.J., 2000. Isotopic evidence for variations in the marine calcium cycle over the Cenozoic. Science 289, 1176-1178.

DePaolo D. J., 2011. Surface kinetic model for isotopic and trace element fractionation during precipitation of calcite from aqueous solutions. Geochim. Cosmochim. Acta 75, 1039–1056.

Dickson, J.A.D., Wood, R.A., Bu Al Rougha, H., and Shebl, H., 2008. Sulphate reduction associated with hardgrounds: Lithification afterburn! Sedimentary Geology, 205, 34-39.

Dravis, J., 1979. Rapid and widespread generation of Recent oolitic hardgrounds on a high energy Bahamian platform, Eleuthera bank, Bahamas. J. Sediment. Petrol. 49, 195–207.

Fantle, M.S., 2010. Evaluating the Ca Isotope Proxy. American Journal of Science, 310, 194-230. Doi:10.2475/03.2010.03.

Fantle M. S., 2015. Calcium isotopic evidence for rapid recrystallization of bulk marine carbonates and implications for geochemical proxies. Geochim. Cosmochim. Acta, 148, 378–401.

Fantle, M.S., and DePaolo, D.J., 2005. Variations in the marine Ca cycle over the past 20 million years: Earth Planet. Sci. Lett., v. 237, p. 102–117, doi:10.1016/j.epsl.2005.06.024.

Fantle, M.S., DePaolo, D.J., 2007. Ca isotopes in carbonate sediment and pore fluid from ODP Site 807A: The $Ca^{2+}_{(aq)}$-calcite equilibrium fractionation factor and calcite recrystallization rates in Pleistocene sediments. Geochim. Cosmochim. Acta 71, 2524-2546.

Fantle, M.S., Maher, K.M., DePaolo, D.J., 2010. Isotopic approaches for quantifying the rates of marine burial diagenesis. Rev. Geophys., 48, RG3002.

Fantle, M.S., Tipper, E.T., 2014. Calcium isotopes in the global biogeochemical Ca cycle: Implications for development of a Ca isotope proxy. Earth-Science Reviews, 129, 148-177.

Farkaš, J., Böhm, F., Wallmann, K., Blenkinsop, J., Eisenhauer, A., van Geldern, R., Munnecke, A., Voigt, S., and Veizer, J., 2007a. Calcium isotope record of Phanerozoic oceans: Implications for chemical evolution of seawater and its causative mechanisms: Geochim. Cosmochim. Acta, v. 71, p. 5117–5134, doi:10.1016/j.gca.2007.09.004.

Farkaš, J., Buhl, D., Blenkinsop, J., and Veizer, J., 2007b. Evolution of the oceanic calcium cycle during the late Mesozoic: Evidence from δ44/40Ca of marine skeletal carbonates: Earth Planet. Sci. Lett., v. 253, p. 96–111, doi:10.1016/j.epsl.2006.10.015.

Friedman, G.M., 1965. Relationships of aragonite, high-magnesian calcite, and low-magnesian calcite under deep sea conditions. GSA Bulletin 76, 1191-1196.

Gothman, A.M., Bender. M.L., Blättler, C.L., Swart, P.K., Giri, S.J., Adkins, J.F., Stolarski, J., Higgins, J.A., 2016. Calcium isotopes in scleractinian fossil corals since the Mesozoic: Implications for vital effects and biomineralization through time. Earth Planet. Sci. Lett., 444, 205-214.

Griffith, E.M., Paytan, A., Caldeira, K., Bullen, T.D., Thomas, E., 2008. A dynamic marine calcium cycle during the past 28 million years: Science, v. 322, p. 1671–1674, doi:10.1126/science.1163614.

Griffith, E.M., Fantle, M.S., Eisenhauer, A., Paytan, A., Bullen, T.,D., 2015. Effects of ocean acidification on the marine calcium isotope record at the Paleocene-Eocene Thermal Maximum. Earth Planet. Sci. Lett. 419, 81-92.

Gussone, N., Eisenhauer, A., Heuser, A., Dietzel, M., Bock, B., Böhm, F., Spero, H.J., Lea, D.W., Bijma, J., and Nägler, T.F., 2003. Model for kinetic effects on calcium isotope fractionation (δ44Ca) in inorganic aragonite and cultured planktonic foraminifera. Geochim. Cosmochim. Acta, v. 67, p. 1375–1382, doi:10.1016/S0016-7037(02)01296-6.

Gussone, N., Böhm, F., Eisenhauer, A., Dietzel, M., Heuser, A., Teichert, B.M.A., Reitner, J., Wörheide, G., and Dullo, W.-C., 2005, Calcium isotope fractionation in calcite and aragonite: Geochim. Cosmochim. Acta, v. 69, p. 4485–4494, doi:10.1016/j.gca.2005.06.003.

Heuser, A., Eisenhauer, A., Böhm, F., Wallmann, K., Gussone, N., Pearson, P.N., Nägler, T.F., and Dullo, W.C., 2005. Calcium isotope ($\delta^{44/40}$Ca) variations of Neogene planktonic foraminifera: Paleoceanography, v. 20, PA2013, doi:10.1029/2004PA001048.

Higgins, J.A., Blättler, C.L., Lundstrom, E.A., Santiago-Ramos, D.P., Akhtar, A.A., Ahm, A.S.C., Bialik, O., Holmden, C., Bradbury, H., Murray, S.T., Swart, P.K., 2018. Mineralogy, early marine diagenesis, and the chemistry of shallow-water carbonate sediments. Geochim. Cosmochim. Acta 220, 512-534.

Hippler, D., Eisenhauer, A., Nägler, T.F., 2006. Tropical Atlantic SST history inferred from Ca isotope thermometry over the last 140 ka. Geochim. Cosmochim. Acta 70, 90–100.

Huber, C., Druhan, J. L., Fantle, M.S., 2017. Perspectives on geochemical proxies: the impact of model and parameter selection on the quantification of carbonate recrystallization rates. Geochim. Cosmochim. Acta 217, 171–192.

Immenhauser, A., Nägler, T.F., Steuber, T., Hippler, D., 2005. A critical assessment of mollusk 18O/16O, Mg/Ca, and 44Ca/40Ca ratios as proxies for Cretaceous seawater temperature seasonality. Palaeogeogr. Palaeoclimatol. Palaeoecol. 215, 221–237.

Kang, J.T., Ionov, D.A., Liu, F., Zhang, C-L., Golovin, A.V., Qin, L-P., Zhang, Z-F., Huang, F., 2017. Calcium isotope fractionation in mantle peridotites by melting and metasomatism and Ca isotope composition of the Bulk Silicate Earth. Earth Planet, Sci. Lett, 474, 128-137.

Kasemann, S.A., Hawkesworth, C., Prave, A.R., Fallick, A.E., Pearson, P.N., 2005. Boron and calcium isotope composition in Neoproterozoic carbonate rocks from Namibia: evidence for extreme environmental change. Earth Planet. Sci. Lett. 231, 73–86.

Kasemann, S.A., Pogge von Strandmann, P.A.E., Prave, A.R., Fallick, A.E., Elliott, T., Hoffmann, K.H., 2014. Continental weathering following a Cryogenian glaciation: evidence from calcium and magnesium isotopes. Earth Planet. Sci. Lett. 396, 66–77. dx.doi.org/10.1016/j.epsl.2014.03.048.

Kennedy, W.J., Garrison, R.E., 1975. Morphology and genesis of nodular chalks and hardgrounds in the Upper Cretaceous of southern England. Sedimentology 22, 311 –386.

Khalaf, F., Milliman, J.D., Druffel, E.M., 1987. Submarine limestones in the nearshore environment off Kuwait, northern Arabian Gulf. Sedimentology 34, 67–75.

Lemarchand, D., Wasserburg, G., Papanastassiou, D., 2004. Rate-controlled calcium isotope fractionation in synthetic calcite. Geochim. Cosmochim. Acta 68, 4665–4678.

Lighty, R.G., 1985. Preservation of internal reef porosity and diagenetic sealing of submerged early Holocene Barrier Reef, SE Florida Shelf. In: Harris, S.A. (Ed.), Carbonate Cements. SEPM, pp. 123–151.

Malone, M.J., Slowey, N.C., Henderson, G.M., 2001. Early diagenesis of shallow-water periplatform carbonate sediments, leeward margin, Great Bahama Bank (Ocean Drilling Program Leg 166). GSA Bull. 113, 881–894.

Marriott, C.S., Henderson, G.M., Belshaw, N.S., and Tudhope, A.W., 2004. Temperature dependence of δ^7Li, δ^{44}Ca and Li/Ca during growth of calcium carbonate. Earth Planet. Sci. Lett., 222, 615–624, doi:10.1016/j.epsl.2004.02.031.

Nägler, T., Eisenhauer, A., Muller, A., Hemleben, C., Kramers, J., 2000. The δ^{44}Ca temperature calibration on fossil and cultured Globigerinoides sacculifer: new tool for reconstruction of past sea surface temperatures. Geochem. Geophys. Geosyst. 1 (2000GC000091).

Nielsen L. C., DePaolo D. J., De Yoreo J. J., 2012. Self consistent ion-by-ion growth model for kinetic isotopic fractionation during calcite precipitation. Geochim. Cosmochim. Acta 86, 166–181.

Payne, J.L., Turchyn, A.V., Paytan, A., DePaolo, D.J., Lehrmann, D.J., Yu, M., Wei, J., 2010. Calcium isotope constraints on the end- Permian mass extinction. National Academy of Sciences Proceedings, 107, 8543–8548, doi:10.1073/pnas.0914065107.

Pruss, S.D., Blättler, C.L., Macdonald, F.A., Higgins, J.A., 2018. Calcium isotope evidence that the earliest metazoan biomineralizers formed aragonite shells. Geology 46, 763-766.

Rameil, N., Immenhauser, A., Csoma, A., Warrlich, G., 2012. Surfaces with a long history: the Aptian top Shu'aiba Formation unconformity, Sultanate of Oman. Sedimentology 59, 212–248.

Ridgwell, A., 2005. A Mid Mesozoic Revolution in the regulation of ocean chemistry. Marine Geology, 217, 339-357.

Ridgwell A., Zeebe, R.E. 2005. The role of the global carbonate cycle in the regulation and evolution of the Earth system. Earth Planet. Sci. Lett. 234, 299-315.

Shinn, E.A., 1969. Submarine lithification of Holocene carbonate sediments in the Persian Gulf. Sedimentology 12, 109–144.

Schmitt, A.-D., Stille, P., Vennemann, T., 2003. Variations of the $^{44}Ca/^{40}Ca$ ration in seawater during the past 24 million years: evidence from $\delta^{44}Ca$and $\delta^{18}O$values of Miocene phosphates. Geochim. Cosmochim. Acta 67, 2607–2614.

Sime, N.G., De La Rocha, C.L., Galy, A., 2005. Megligible temperature dependence of calcium isotope fractionation in 12 species of planktonic foraminifera. Earth and Planetary Science Letters, 232,51-66, doi: 10.1016/j.epsl.2005.01.011.

Sime, N.G., De La Rocha, C.L., Tipper, E.T., Tripati, A., Galy, A., Bickle, M.J., 2007. Interpreting the Ca isotope record of marine biogenic carbonates. Geochimica et Cosmochimica Acta, v. 71, p. 3979–3989, doi:10.1016/j.gca.2007.06.009.

Soudry, D., Segal, I., Nathan, Y., Glenn, C.R., Halicz, L., Lewy, Z., VonderHaar, D.L., 2004. $^{44}Ca/^{42}Ca$ and $^{143}Nd/^{144}Nd$ isotope variations in Cretaceous–Eocene Tethyan francolites and their bearing on phosphogenesis in the southern Tethys. Geology 32, 389–392.

Soudry, D., Glenn, C.R., Nathan, Y., Segal, I., VoderHaar, D.L., 2006. Evolution of Tethyan phosphogenesis along the northern edges of the Arabian–African shield during the Cretaceous–Eocene as deduced from temporal variations of Ca and Nd isotopes and rates of P accumulation. Earth-Sci. Rev.78, 27–57.

Stanley, S.M., Hardie, L., 1998. Secular oscillations in the carbonate mineralogy of reef-building and sediment-producing organisms driven by tectonically forced shifts in seawater chemistry: Palaeogeography, Palaeoclimatology, Paleoecology, 144, 3–19, doi:10.1016/S0031-0182(98)00109-6.

Steuber, T., Buhl, D., 2006. Calcium-isotope fractionation in selected modern and ancient marine carbonates. Geochim. Cosmochim. Acta, 70, 5507–5521.

Tang, J., Deitzel, M., Böhm, F., Köhler, S.J., Eisenhauer, A., 2008. Sr^{2+}/Ca^{2+} and $^{44}Ca/^{40}Ca$ fractionation during inorganic calcite formation: II. Ca isotopes. Geochim. Cosmochim. Acta 72, 3733-3745.

Teichert, B.M.A., Gussone, N., Torres, M.E., 2009. Controls on calcium isotope fractionation in sedimentary porewaters. Earth Planet. Sci. Lett. 279, 373–382.

Tostevin, R., Shields, G.A., Tarbuck, G.M., He, T., Clarkson, M.O., Wood, R.A., 2016. Effective use of cerium anomalies as a redox proxy in carbonate-dominated marine settings. Chemical Geology 438, 146–162.

Turchyn A. V. DePaolo D. J., 2011. Calcium isotope evidence for suppression of carbonate dissolution in carbonate-bearing organic-rich sediments. Geochim. Cosmochim. Acta 75, 7081– 7098.

C.G. Weinzierl, C.G., Regelous, M., Haase, K.M., Bach, W., Böhm, F., Garbe-Schönberg, D., Sun, Y.D., Joachimski, M.M., Krumm, S., 2018. Cretaceous seawater and hydrothermal fluid compositions recorded in abiogenic carbonates from the Troodos Ophiolite, Cyprus. Chemical Geology, 494, 43-55.

Zhuravlev, A.Y., Wood, R.A., 2009. Controls on carbonate skeletal mineralogy: Global CO2 evolution and mass extinctions. Geology, 37, 1123-1126, doi 10.1130/G30204A.1.